Quiet T1-weighted 3D Imaging of the Central Nervous System Using PETRA

Masahiro Ida, M.D.[1]; Matthew Nielsen, M.A.[2]

[1]Dept. of Radiology, Tokyo Metropolitan Ebara Hospital, Tokyo, Japan
[2]Research & Collaboration Dept., Healthcare Sector, Siemens Japan K.K., Tokyo, Japan

Introduction

Nearly all MRI sequences in routine clinical use employ rapidly varying magnetic field gradients that generate considerable acoustic noise, one of the primary causes of patient discomfort and restlessness [1]. Eliminating such noise would provide additional comfort for all patients, and may provide particular advantages for patients with pediatric*, dementia and certain psychiatric diseases who tend to have difficulty relaxing or remaining still during MR examinations.

Ultra-short echo time sequences such as zero-TE [2], SWIFT [3] and PETRA [4] require only limited gradient activity and allow for inaudible 3D scanning. However, due to ultra-short TEs, the image contrast is given by the steady state and is limited to the range of PD- to T1-weighting unless pre-pulses are used [5]. Similar to the MPRAGE sequence [6-8], stronger T1-weighting can be generated by applying an inversion pre-pulse before every n^{th} repetition in the PETRA* sequence. A study has shown that this quiet inversion-prepared PETRA sequence is capable of T1-weighting comparable to that of MPRAGE when measured in the same time and with the same spatial resolution [1].

In this article, examples of quiet inversion-prepared PETRA images are compared with conventional 3D T1-weighted images (MPRAGE or 3D-FLASH) from the same patients. All of the examples were obtained during brain examinations, and all but one of the examples employed contrast enhancement.

* WIP, the product is currently under development and is not for sale in the US and other countries. Its future availability cannot be ensured.

PETRA sequence principles and noise reduction

In the PETRA sequence, gradients are already on and stable at a certain amplitude before the excitation pulse, as shown in figure 1. At the end of each repetition, the gradient strength on each axis is altered only slightly meaning that the required slew rate is extremely low (e.g., < 5 T/m/s with

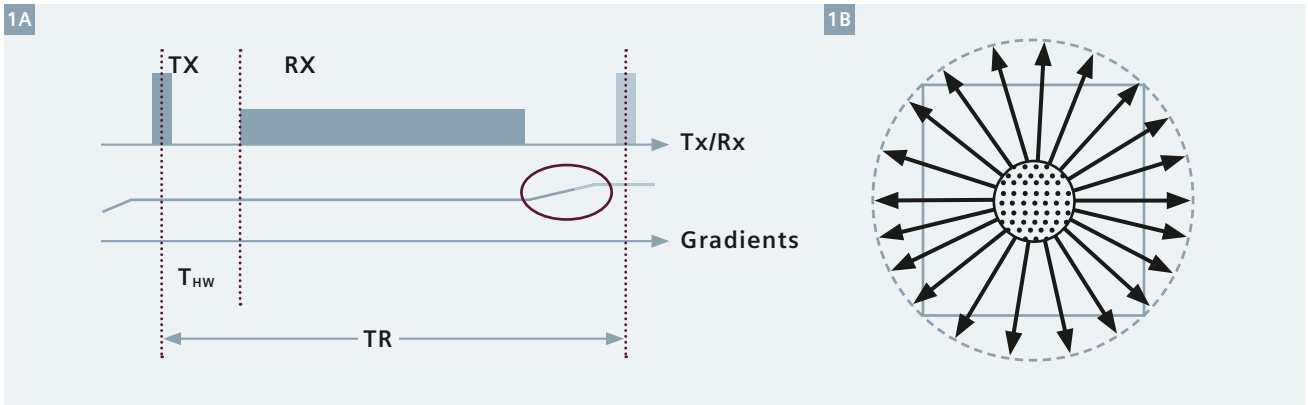

1 PETRA combines two different sequences, acquiring central *k*-space in a 'point-wise' fashion (one *k*-space point per repetition), and the rest of *k*-space with radial trajectories. PETRA stands for Pointwise Encoding Time reduction with Radial Acquisition. No hardware modifications or dedicated coils are needed [1].
(1A) Pulse sequence diagram for one repetition of the radial part of the PETRA sequence. Gradients are held constant during almost an entire repetition and altered only slightly at the end of each repetition without being ramped down. This leads to negligible deformation and vibration of the gradient coil. Thus, no acoustic noise is generated by the gradient coil. T_{HW} is the time required to switch from transmission mode to receive mode (in the range of 10 to 100 μs on clinical scanners) [1].
(1B) During T_{HW}, a spherical volume (dots) at the center of *k*-space is missed by the radial part of the sequence. Each *k*-space point inside that spherical volume is acquired separately in the Pointwise Encoding (PE) part of the sequence. The acquisition time of the PE part is approximately 3 to 5% of the total measurement time [1].

PETRA) [1]. The resulting deformation and vibration of the gradient coil is negligible and produces almost no audible sound. Completely unrelated to the gradients however, transmit-mode-to-receive-mode switching (and vice versa) in receive-only RF coils produces some noise [1], while PETRA is essentially inaudible when used with transmit-and-receive RF coils.

The acoustic noise levels generated by PETRA and MPRAGE on a MAGNETOM Trio A Tim System (3T) were measured using a sound-pressure meter with A-weighting. PETRA afforded a reduction in acoustic noise of more than 25 dB_A with both the 12-channel head matrix coil and the 32-channel head coil. Since both coils were receive-only, an even greater reduction can be expected with transmit-and-receive coils.

PETRA versus routine sequence image comparisons

While MR angiography (MRA) is undoubtedly the most commonly-used 3D sequence in brain MRI exams, other 3D sequences are used in certain circumstances at Tokyo Metropolitan Ebara Hospital. The most common one is contrast-enhanced (CE) 3D-FLASH which is employed for the following indications because of its high spatial resolution and short echo time:

(1) To precisely diagnose head & neck tumors, pre- & post-operatively (with Quick FatSat),
(2) to inspect blood pools (AVM, thrombosis, aneurysm, dissection), and
(3) to detect cranial nerve inflammation.

The second most common 3D scan other than MRA is CE MPRAGE which is employed to diagnose intracranial brain tumors. Among those, the most common indication is screening for intracranial metastases.

MR imaging was performed on a 3 Tesla MAGNETOM Trio A Tim System. PETRA was added to routine patient exams that included either MPRAGE or 3D-FLASH. The parameters of the three sequences are shown in table 1.

The center of *k*-space for MPRAGE (scan time: 5 min 56 sec) was acquired approximately 6 to 11 minutes after contrast media administration, while the center of *k*-space for PETRA was acquired approximately 3 minutes later than that of MPRAGE, 9 to 14 minutes after contrast media administration. PETRA acquires the central portion of *k*-space first (in a pointwise fashion as shown in figure 1) before acquiring the rest of 3D *k*-space with radial trajectories. A previous study showed that for enhancing intracranial lesions with a diameter of 5 mm or larger, enhancement reached a plateau in less than 10 minutes and lasted until at least 20 minutes after contrast media injection [9]. Thus, the 3 minute difference in the acquisition of $k = 0$ between MPRAGE and PETRA would not result in differing lesion enhancement, and any difference in lesion enhancement can be taken as primarily due to sequence characteristics.

Protocols provided with the PETRA sequence were designed to parallel the contrast and spatial resolution (0.9 to 1.0 mm cubic voxels) typically available with MPRAGE. Therefore, initial work with PETRA at our hospital focused on comparisons with MPRAGE. One of the protocols placed the priority on signal-to-noise ratio (SNR) (TI 900 ms), and one placed the priority on contrast-to-noise ratio (CNR) (TI 500 ms, for higher contrast between gray matter (GM) and white matter (WM)).

The scan times of both PETRA protocols were adjusted such that they were similar to that of the MPRAGE protocol used in patient exams. In a pilot study, volunteers and patients were scanned with both PETRA protocols and with

Table 1: Sequence parameters

	PETRA Figs. 2, 3, 11, 12	PETRA Figs. 4–10	MPRAGE Figs. 2–8	3D-FLASH Figs. 9–12
Voxel size / mm	$(0.99\ mm)^3$ for Figs. 2,3 $(0.80\ mm)^3$ for Figs. 11, 12	$(0.99\ mm)^3$	$(0.94\ mm)^3$	$0.6 \times 0.6 \times 1.0\ mm^3$
Matrix	288 × 288	288 × 288	256 × 256	346 × 384
Slices	288	288	176	144
TI / ms	500 for Figs. 2, 3 900 for Figs. 11, 12	700	900	n.a.
TR / ms	2.79	2.79	5.6[1]	11
TE / ms	0.07	0.07	2.4	6.2
FA / deg	6	6	10	20
FatSat	No	Yes	No	Yes
Scan time	05:59	06:20	5:56 (3:54 for Fig. 2)	02:52

[1]Repetition time of RF excitation pulses, which for MPRAGE is displayed on the MR console as 'Echo spacing'.

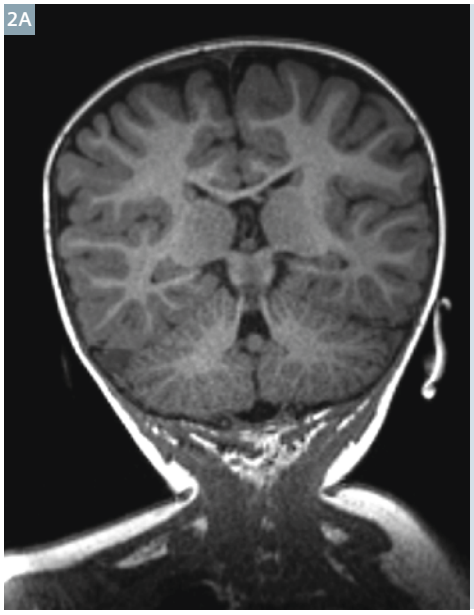

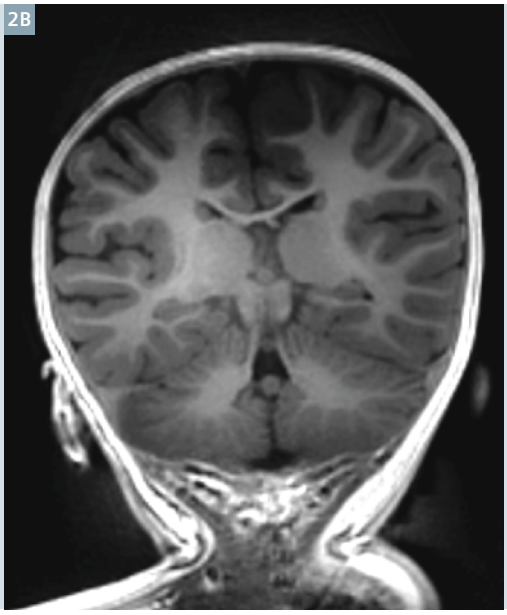

2

MR imaging was indicated for a 19-month-old* female experiencing seizures with no associated fever. Neither sequence revealed any brain abnormality. **(2A)** MPRAGE, **(2B)** CE PETRA with a TI of 500 ms demonstrated excellent gray-to-white-matter contrast comparable with that of MPRAGE.

* MR scanning has not been established as safe for imaging fetuses and infants less than two years of age. The responsible physician must evaluate the benefits of the MR examination compared to those of other imaging procedures.

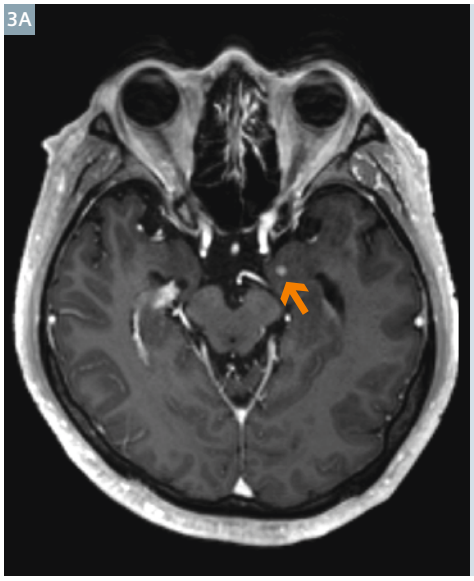

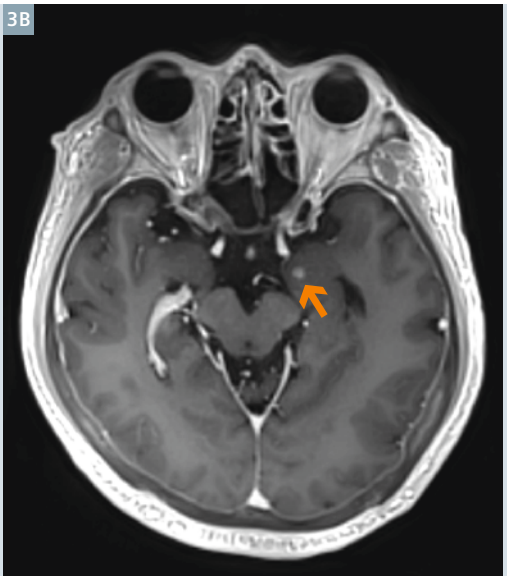

3

Contrast-enhanced screening for brain metastases was indicated for a 57-year-old male who had lung cancer. A tiny metastasis (diameter 3.5 mm) was detected in the medial portion of the left temporal lobe (arrows) on both sequences.
(3A) CE MPRAGE,
(3B) CE PETRA with an inversion time of 500 ms.

MPRAGE. The SNR on PETRA images with TI 900 ms was visibly higher than on MPRAGE images, while PETRA images with TI 500 ms provided more GM-to-WM contrast than necessary for CE studies in the opinion of one radiologist (MI). A decision was made that some of the SNR could be 'traded for' tissue CNR, and an intermediate TI of 700 ms was chosen for further CE studies. Statistical comparisons of contrast enhancement and SNR between PETRA and MPRAGE were performed (that study is under review for publication in a peer-reviewed journal).

PETRA was also compared with 3D-FLASH while remaining conscious of the fact that, compared to the PETRA implementation discussed in this article, 3D-FLASH was capable of higher spatial resolution.

Clinical observations

Comparisons of PETRA and MPRAGE

Comparisons between PETRA and MPRAGE with similar spatial resolution and without fat suppression are shown in figures 2 and 3. GM-to-WM contrast is seen to be similar, both without (Fig. 2) and with (Fig. 3) contrast enhancement (CE). In the latter CE case, a small enhancing lesion appears to have the same size and enhancement on the PETRA image as on the MPRAGE image.

The remaining comparisons between PETRA and MPRAGE, figures 4 through 8, were contrast-enhanced studies of intracranial primary or metastatic tumors with the same resolution parameters as above. However, two PETRA parameters were modified: TI was changed to 700 ms, sacrificing some GM-to-WM contrast for a gain in SNR, and fat-suppression was added (to PETRA only, avoiding a change to the hospital's routine MPRAGE protocol).

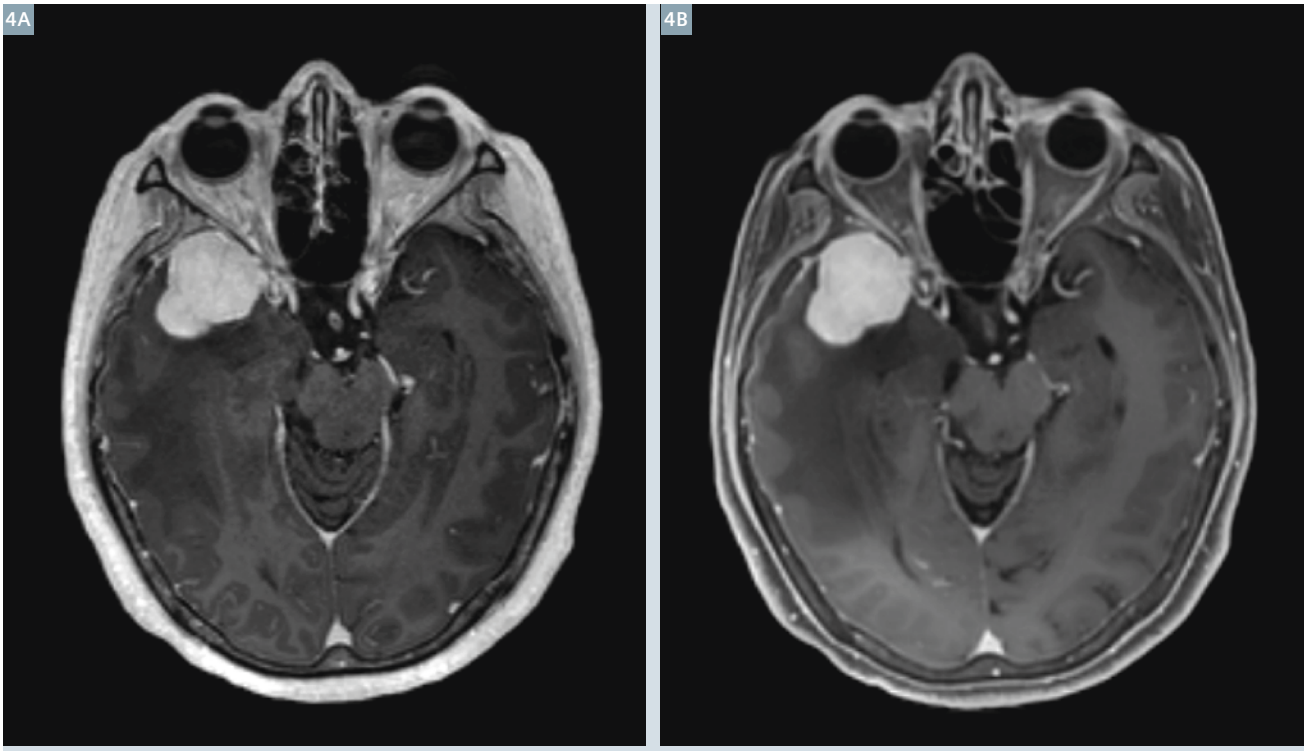

4 Contrast-enhanced images of gliobastoma in a 56-year-old female patient (not proven histologically).
(4A) CE MPRAGE, **(4B)** fat-suppressed CE PETRA.

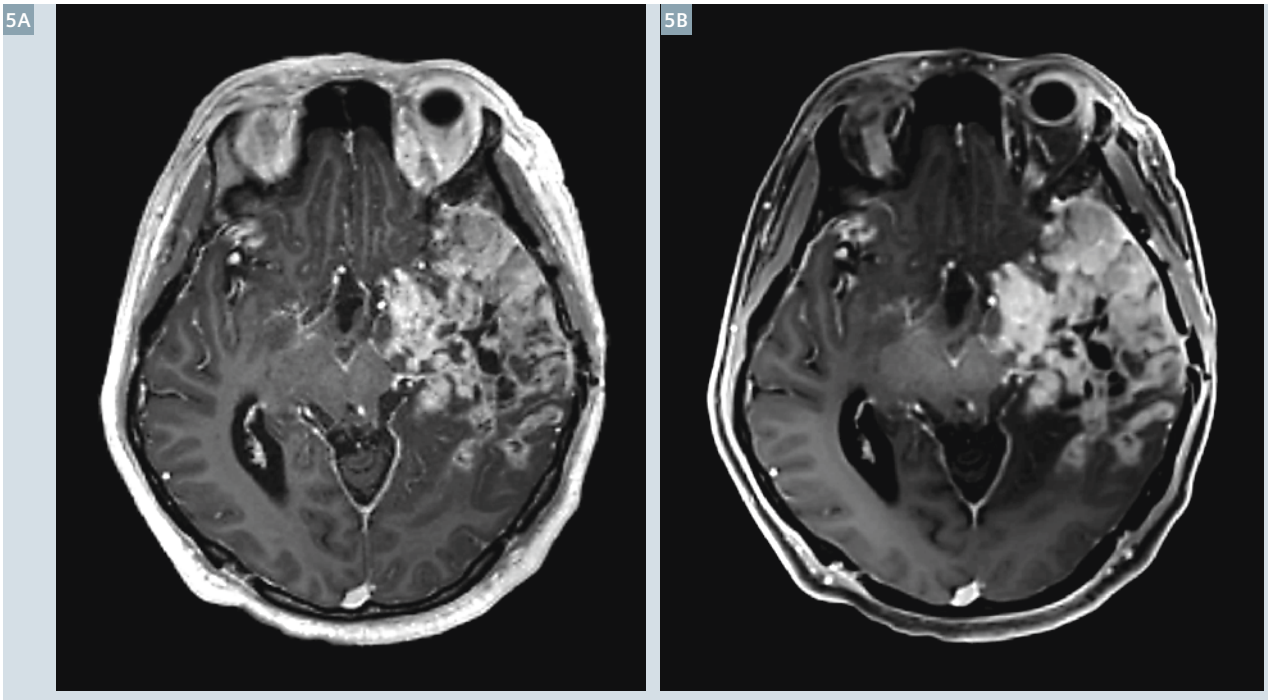

5 Contrast-enhanced images of glioblastoma in a 33-year-old male patient.
(5A) CE MPRAGE, **(5B)** fat-suppressed CE PETRA.

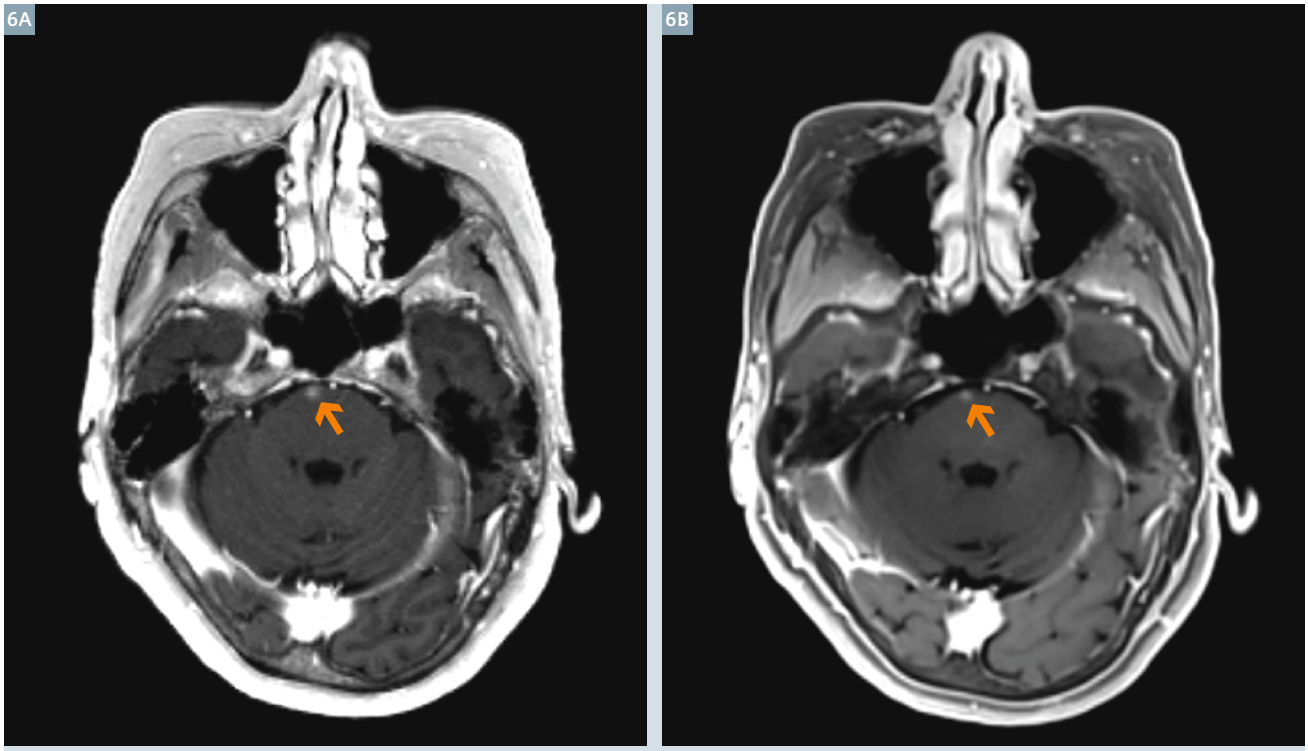

6 Contrast-enhanced screening for brain metastases was indicated for a 70-year-old female who had lung cancer. A small metastasis was detected in the supependymal zone of the pons (arrows) on both sequences. **(6A)** CE MPRAGE, **(6B)** fat-suppressed CE PETRA.

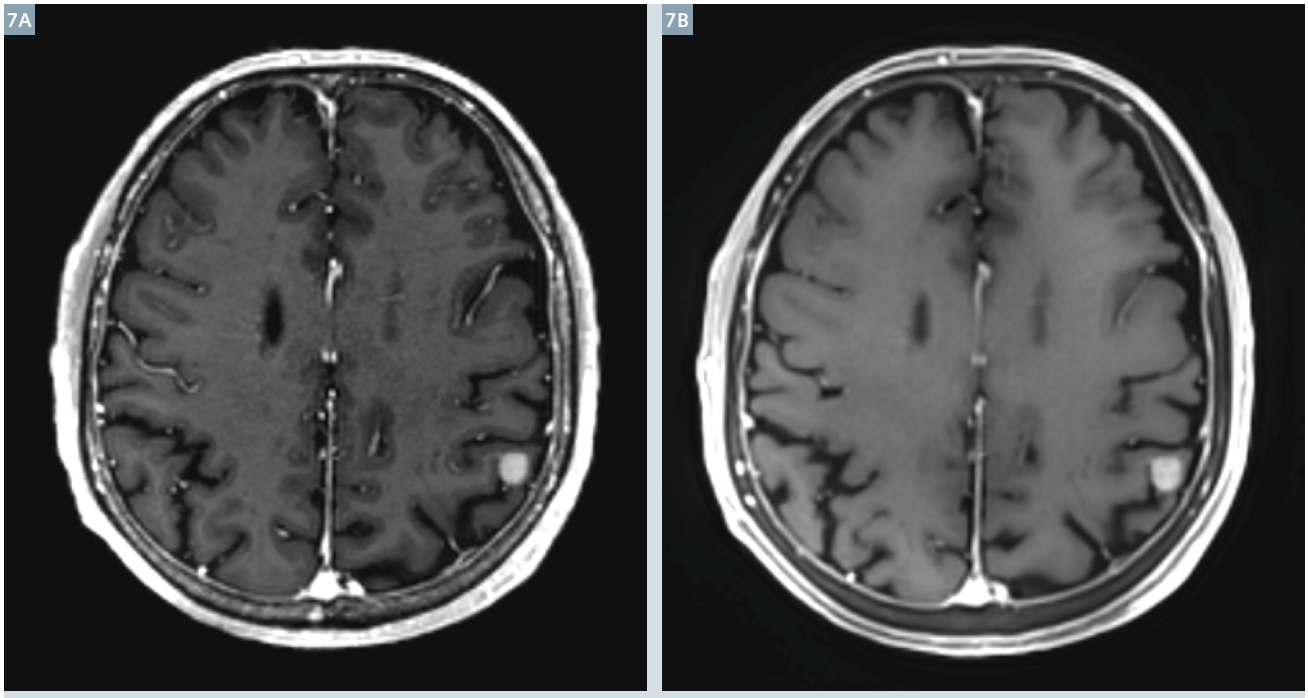

7 Contrast-enhanced screening for brain metastases was indicated for a 69-year-old male who had lung cancer. A small metastasis was detected in the corticomedullary junction of the left parietal lobe on both sequences. **(7A)** CE MPRAGE, **(7B)** fat-suppressed CE PETRA.

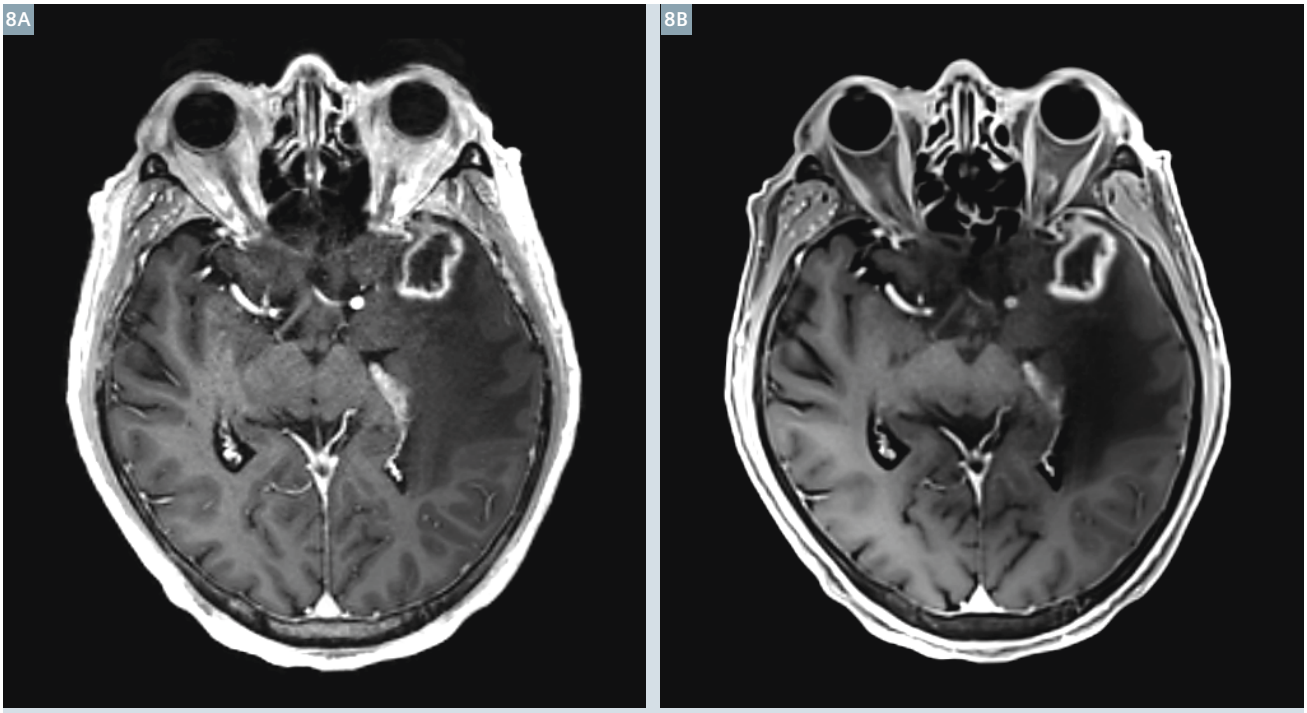

8 Contrast-enhanced screening for brain metastases was indicated for a 63-year-old male. A ring-enhancing lesion was detected in the left temporal lobe on both sequences. **(8A)** CE MPRAGE, **(8B)** fat-suppressed CE PETRA.

Comparisons of PETRA and 3D-FLASH

Comparisons between PETRA and 3D-FLASH are shown in figures 9 through 12. While the acquired spatial resolution was higher for 3D-FLASH ($0.6 \times 0.6 \times 1.0$ mm^3) than for PETRA, the clinical findings were not affected in these cases. PETRA had a voxel size of 0.993 mm^3 (Figs. 9, 10) or 0.803 mm^3 (Figs. 11, 12).

General clinical observations

Susceptibility-related artifacts and flow voids were absent on PETRA images, while signal from cortical bone was observed. All three observations can be attributed to the ultra-short TE. The absence of susceptibility-related artifacts should allow PETRA to detect sinusitis or tumors within the paranasal sinsuses which tend to be highly distorted on 3D gradient-echo-based sequences such as MPRAGE and 3D-FLASH. Positive signal from bone may be useful in cases of head trauma for detecting fractures and in surgical planning and follow-up. While CT is normally used for this purpose in adults, its use is highly restricted in children. PETRA may be able to readily provide 3D bone images even for children, or to provide more frequent follow-ups after surgery in adults.

The masticator space and the paranasal space at the skull base tended to appear 'dirty' or 'messy' on PETRA images, but this was not the result of an artifact or distortion. Rather, this appearance was caused by strong venous enhancement due to the absence of flow voids. Also on PETRA, the dura mater as well as the mucosa in the paranasal sinuses exhibited contrast enhancement, and the enhancement of the dura was uniform in most cases. This was likely due to blood pool enhancement in capillary arteries which are dense in those tissues, in combination with the absence of flow voids as a result the ultra-short TE. Such enhancement did not appear on MPRAGE and 3D-FLASH images. The uniform enhancement of the dura would prevent the use of PETRA for the detection of dural inflammation, dural metastasis, intracranial hypotension or other causes of local dural enhancement. Nevertheless, many other applications of 3D T1-weighted imaging exist such as those presented in the current article.

Finally, PETRA demonstrated excellent fat suppression which would allow the sequence to be employed, not only for the diagnosis of intracranial tumors, but also for the diagnosis of extracranial, orbital and paranasal tumors including bone-marrow metastases of the calvaria and cranial base.

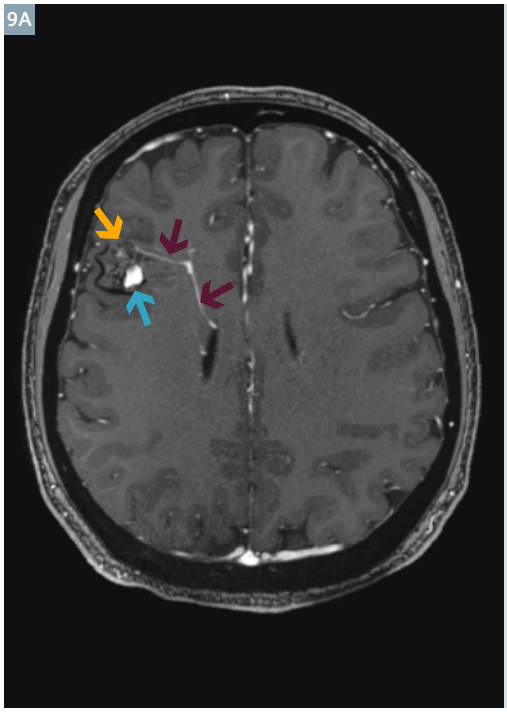

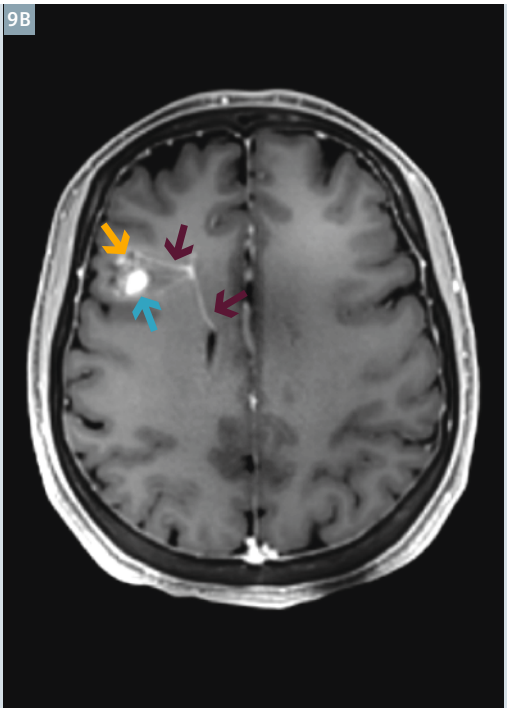

9

Contrast-enhanced images of dilated, abnormal medullary veins representing developmental venous anomaly **(red arrows)** in a 47-year-old female patient. **Yellow arrows:** Small blood pool enhancement in the combined cavernous malformation.
Blue arrows: T1 shortening caused by methemoglobin.
(9A) CE 3D-FLASH with a voxel size of 0.6 × 0.6 × 1.0 mm^3.
(9B) CE PETRA (TI 700 ms) with a voxel size of (0.99 $mm)^3$.

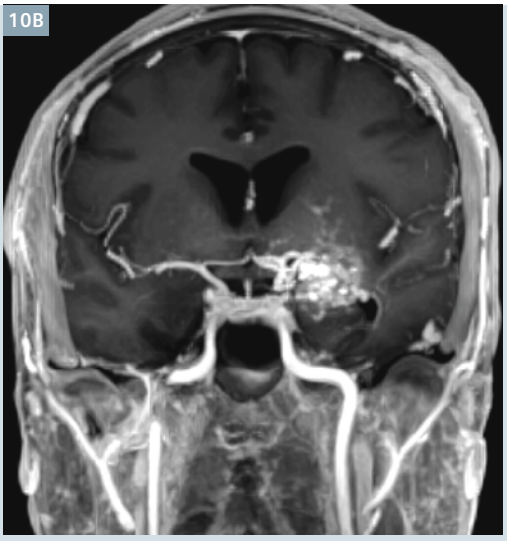

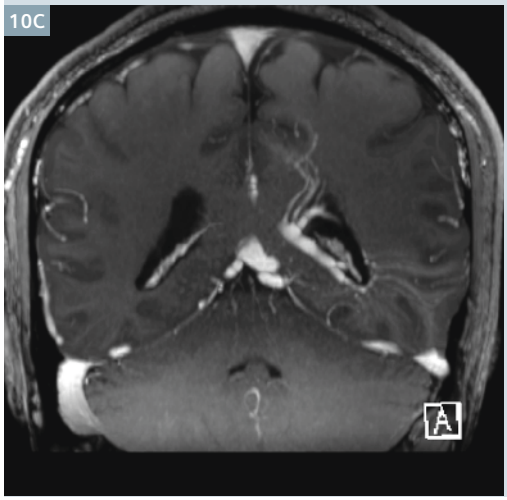

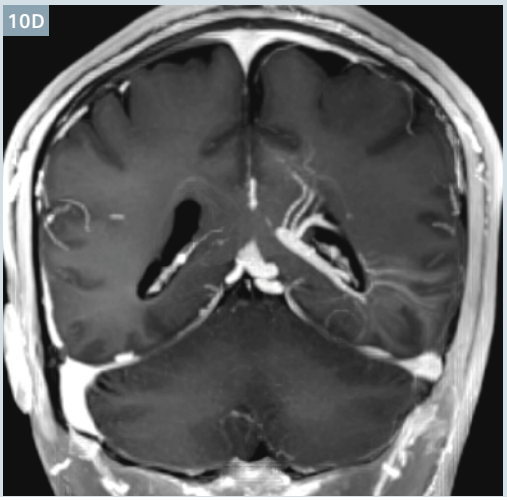

10

Contrast-enhanced images of combined cavernous malformation and developmental venous anomaly in a 47-year-old female patient.
(10A) CE 3D-FLASH with a voxel size of 0.6 × 0.6 × 1.0 mm^3.
(10B) CE PETRA (TI 700 ms) with a voxel size of (0.99 $mm)^3$.
Flow voids are absent due to the ultra-short TE causing the venous malformation to appear more prominently.
Developmental venous malformation was apparent in the same patient, again appearing more prominently on PETRA due to the ultra-short TE and lack of flow voids.
(10C) CE 3D-FLASH.
(10D) CE PETRA.

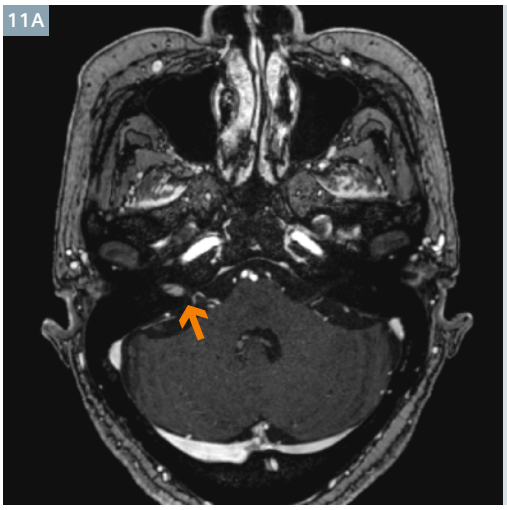

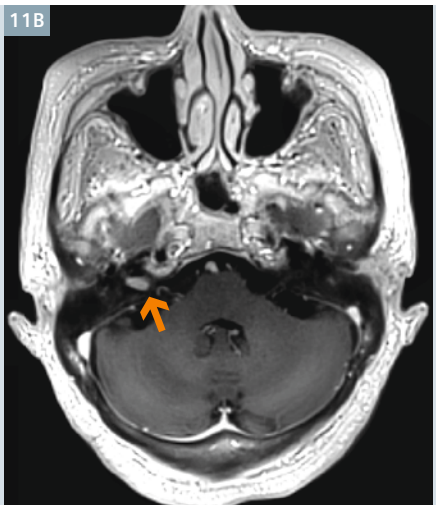

11

Contrast-enhanced images of small vestibular schwannoma (arrows) localized in the right acoustic canal of a 67-year-old female patient.
(11A) CE 3D-FLASH with a voxel size of 0.6 × 0.6 × 1.0 mm³.
(11B) CE PETRA (TI 900 ms) with a voxel size of (0.80 mm)³.

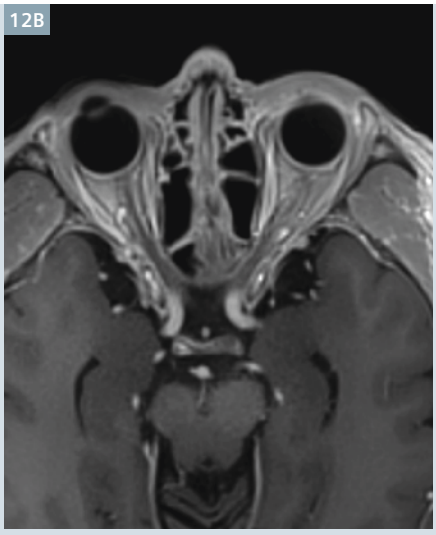

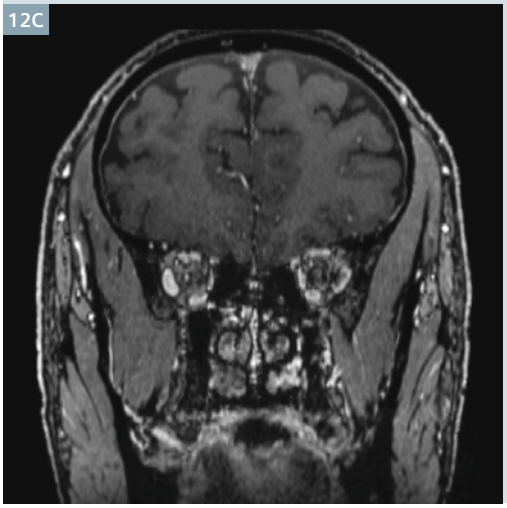

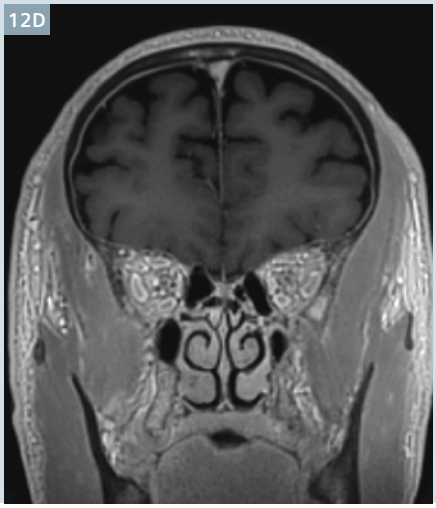

12

Normal optic nerves and paranasal sinuses in a 74-year-old male patient.
(12A) 3D-FLASH with a voxel size of 0.6 × 0.6 × 1.0 mm³.
(12B) PETRA (TI 900 ms) with a voxel size of (0.80 mm)³.
The septi of the paranasal sinuses are depicted clearly in the ethmoid sinuses due to the absence of susceptibility-induced artifacts.

Normal paranasal sinuses in the same patient.
(12C) 3D-FLASH.
(12D) PETRA. Notice the absence of susceptibility-induced artifacts in the paranasal sinus.

Conclusion

The acoustic noise (A-weighted) generated by PETRA was drastically lower than that of MPRAGE, while contrast-enhancement and image quality were similar between the two sequences, and clinical findings did not differ, as shown in several examples. In comparisons of PETRA with 3D-FLASH, although the latter provided a higher spatial resolution, again clinical findings did not differ. Quieter MRI examinations will be more comfortable for all patients, and may have particular advantages for pediatric, dementia and certain psychiatric patients.

References

1 Grodzki DM, Heismann B. Quiet T1-weighted head scanning using PETRA. Proc ISMRM 2013; 21:0456.
2 Weiger M, Pruessmann KP, Hennel F. MRI with zero echo time: hard versus sweep pulse excitation. Magn Reson Med 2011; 66(2):379-89.
3 Idiyatullin D, Corum C, Park JY, Garwood M. Fast and quiet MRI using a swept radio-frequency. J Magn Reson 2006; 181(2): 342-349.
4 Grodzki DM, Jakob PM, Heismann B. Ultrashort echo time imaging using pointwise encoding time reduction with radial acquisition (PETRA). Magn Reson Med 2012; 67(2):510-508.
5 Chamberlain R, Moeller S, Corum C, Idiyatullin C, Garwood M. Quiet T1- and T2-weighted brain imaging using SWIFT. Proc ISMRM 2011; 19:2723.
6 Mugler JP, Brookeman JR. Three-dimensional magnetization-prepared rapid gradient-echo imaging (3D MP RAGE). Magn Reson Med 1990; 15:152-157.
7 Brant-Zawadzki M, Gillan GD, Nitz WR. MP RAGE: a three-dimensional, T1-weighted, gradient-echo sequence-initial experience in the brain. Radiology 1992; 182:769-75.
8 Brant-Zawadzki MN, Gillan GD, Atkinson DJ, Edalatpour N, Jensen M. Three-dimensional MR imaging and display of intracranial disease: improvements with the MP-RAGE sequence and gadolinium. J Magn Reson Imaging. 1993; 3(4): 656-62.
9 Yuh WT, Tali ET, Nguyen HD, Simonson TM, Mayr NA, Fisher DJ. The effect of contrast dose, imaging time, and lesion size in the MR detection of intracerebral metastasis. AJNR 1995; 16:373-380.

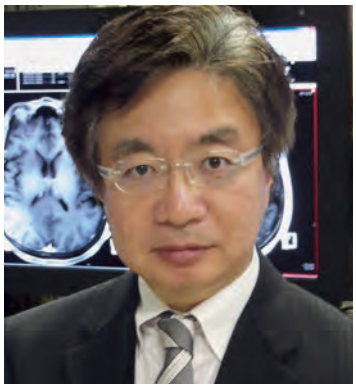

Contact

Masahiro Ida, M.D.
Chief Radiologist
Dept. of Radiology
Tokyo Metropolitan Ebara Hospital
4-5-10 Higashi-yukigaya, Ota-ku
Tokyo 145-0065
Japan
Phone: +81 3-5734-8000
rxb00500@nifty.com